

Observation of TeV gamma rays from the Cygnus region with the ARGO-YBJ experiment

B. Bartoli^{1,2}, P. Bernardini^{3,4}, X.J. Bi⁵, C. Bleve^{3,4}, I. Bolognino^{6,7}, P. Branchini⁸,
 A. Budano⁸, A.K. Calabrese Melcarne⁹, P. Camarri^{10,11}, Z. Cao⁵, R. Cardarelli¹¹,
 S. Catalanotti^{1,2}, C. Cattaneo⁷, S.Z. Chen^{0,5}, T.L. Chen¹², Y. Chen⁵, P. Creti⁴, S.W. Cui¹³,
 B.Z. Dai¹⁴, G. D'Alí Staiti^{15,16}, Danzengluobu¹², M. Dattoli^{17,18,19}, I. De Mitri^{3,4},
 B. D'Ettorre Piazzoli^{1,2}, T. Di Girolamo^{1,2}, X.H. Ding¹², G. Di Sciascio¹¹, C.F. Feng²⁰,
 Zhaoyang Feng⁵, Zhenyong Feng²¹, F. Galeazzi⁸, E. Giroletti^{6,7}, Q.B. Gou⁵, Y.Q. Guo⁵,
 H.H. He⁵, Haibing Hu¹², Hongbo Hu⁵, Q. Huang²¹, M. Iacovacci^{1,2}, R. Iuppa^{10,11},
 I. James^{8,22}, H.Y. Jia²¹, Labaciren¹², H.J. Li¹², J.Y. Li²⁰, X.X. Li⁵, G. Liguori^{6,7}, C. Liu⁵,
 C.Q. Liu¹⁴, J. Liu¹⁴, M.Y. Liu¹², H. Lu⁵, L.L. Ma⁵, X.H. Ma⁵, G. Mancarella^{3,4},
 S.M. Mari^{8,22}, G. Marsella^{4,23}, D. Martello^{3,4}, S. Mastroianni², P. Montini^{8,22}, C.C. Ning¹²,
 A. Pagliaro^{16,24}, M. Panareo^{4,23}, B. Panico^{10,11}, L. Perrone^{4,23}, P. Pistilli^{8,22}, F. Ruggieri⁸,
 P. Salvini⁷, R. Santonico^{10,11}, P.R. Shen⁵, X.D. Sheng⁵, F. Shi⁵, C. Stanescu⁸, A. Surdo⁴,
 Y.H. Tan⁵, P. Vallania^{17,18}, S. Vernetto^{17,18}, C. Vigorito^{18,19}, B. Wang⁵, H. Wang⁵,
 C.Y. Wu⁵, H.R. Wu⁵, B. Xu²¹, L. Xue²⁰, Q.Y. Yang¹⁴, X.C. Yang¹⁴, Z.G. Yao⁵,
 A.F. Yuan¹², M. Zha⁵, H.M. Zhang⁵, Jilong Zhang⁵, Jianli Zhang⁵, L. Zhang¹⁴, P. Zhang¹⁴,
 X.Y. Zhang²⁰, Y. Zhang⁵, J. Zhao⁵, Zhaxiciren¹², Zhaxisangzhu¹², X.X. Zhou²¹,
 F.R. Zhu²¹, Q.Q. Zhu⁵ and G. Zizzi⁹
 (The ARGO-YBJ Collaboration)

⁰Corresponding author: S.Z. Chen, chenzs@ihep.ac.cn

ABSTRACT

¹Dipartimento di Fisica dell’Università di Napoli “Federico II”, Complesso Universitario di Monte Sant’Angelo, via Cinthia, 80126 Napoli, Italy.

²Istituto Nazionale di Fisica Nucleare, Sezione di Napoli, Complesso Universitario di Monte Sant’Angelo, via Cinthia, 80126 Napoli, Italy.

³Dipartimento di Fisica dell’Università del Salento, via per Arnesano, 73100 Lecce, Italy.

⁴Istituto Nazionale di Fisica Nucleare, Sezione di Lecce, via per Arnesano, 73100 Lecce, Italy.

⁵Key Laboratory of Particle Astrophysics, Institute of High Energy Physics, Chinese Academy of Sciences, P.O. Box 918, 100049 Beijing, P.R. China.

⁶Dipartimento di Fisica Nucleare e Teorica dell’Università di Pavia, via Bassi 6, 27100 Pavia, Italy.

⁷Istituto Nazionale di Fisica Nucleare, Sezione di Pavia, via Bassi 6, 27100 Pavia, Italy.

⁸Istituto Nazionale di Fisica Nucleare, Sezione di Roma Tre, via della Vasca Navale 84, 00146 Roma, Italy.

⁹Istituto Nazionale di Fisica Nucleare - CNAF, Viale Berti-Pichat 6/2, 40127 Bologna, Italy.

¹⁰Dipartimento di Fisica dell’Università di Roma “Tor Vergata”, via della Ricerca Scientifica 1, 00133 Roma, Italy.

¹¹Istituto Nazionale di Fisica Nucleare, Sezione di Roma Tor Vergata, via della Ricerca Scientifica 1, 00133 Roma, Italy.

¹²Tibet University, 850000 Lhasa, Xizang, P.R. China.

¹³Hebei Normal University, Shijiazhuang 050016, Hebei, P.R. China.

¹⁴Yunnan University, 2 North Cuihu Rd., 650091 Kunming, Yunnan, P.R. China.

¹⁵Università degli Studi di Palermo, Dipartimento di Fisica e Tecnologie Relative, Viale delle Scienze, Edificio 18, 90128 Palermo, Italy.

¹⁶Istituto Nazionale di Fisica Nucleare, Sezione di Catania, Viale A. Doria 6, 95125 Catania, Italy.

¹⁷Istituto di Fisica dello Spazio Interplanetario dell’Istituto Nazionale di Astrofisica, corso Fiume 4, 10133 Torino, Italy.

¹⁸Istituto Nazionale di Fisica Nucleare, Sezione di Torino, via P. Giuria 1, 10125 Torino, Italy.

¹⁹Dipartimento di Fisica Generale dell’Università di Torino, via P. Giuria 1, 10125 Torino, Italy.

²⁰Shandong University, 250100 Jinan, Shandong, P.R. China.

²¹Southwest Jiaotong University, 610031 Chengdu, Sichuan, P.R. China.

²²Dipartimento di Fisica dell’Università “Roma Tre”, via della Vasca Navale 84, 00146 Roma, Italy.

²³Dipartimento di Ingegneria dell’Innovazione, Università del Salento, 73100 Lecce, Italy.

²⁴Istituto di Astrofisica Spaziale e Fisica Cosmica dell’Istituto Nazionale di Astrofisica, via La Malfa 153,

We report the observation of TeV γ -rays from the Cygnus region using the ARGO-YBJ data collected from 2007 November to 2011 August. Several TeV sources are located in this region including the two bright extended MGRO J2019+37 and MGRO J2031+41. According to the Milagro data set, at 20 TeV MGRO J2019+37 is the most significant source apart from the Crab Nebula. No signal from MGRO J2019+37 is detected by the ARGO-YBJ experiment, and the derived flux upper limits at 90% confidence level for all the events above 600 GeV with medium energy of 3 TeV are lower than the Milagro flux, implying that the source might be variable and hard to be identified as a pulsar wind nebula. The only statistically significant (6.4 standard deviations) γ -ray signal is found from MGRO J2031+41, with a flux consistent with the measurement by Milagro.

Subject headings: gamma rays: general – pulsars: individual (MGRO J2019+37, MGRO J2031+41)

1. Introduction

The Cygnus region is the brightest diffuse γ -ray emitting region in the northern sky as observed by both *Fermi* (Abdo et al. 2011) and EGRET (Hunter et al. 1997). Complex features have been observed in the wavelength bands of radio, infrared, X-rays, and γ -rays. This region is rich in potential cosmic-ray acceleration sites, e.g., Wolf-Rayet stars, OB associations and supernova remnants. Recently, 24 γ -ray sources, including 7 pulsars, have been detected using *Fermi* Large Area Telescope (LAT) two-year data within the region with $65^\circ < l < 85^\circ$ and $-3^\circ < b < 3^\circ$ (Abdo et al. 2011). These are considered candidate sources of very high energy (VHE) γ -rays. The Cygnus region is, therefore, a natural laboratory to study the origin of cosmic rays.

Several VHE γ -ray sources have been detected within the Cygnus region in the past decade. The first was TeV J2032+4130, discovered by the HEGRA collaboration (Aharonian et al. 2002, 2005) and confirmed by the experiments Whipple (Konopelko et al. 2007) and MAGIC (Albert et al. 2008). Its extension is estimated to be about 0.1° . The power-law spectral index is about -2.0 and the integral flux above 1 TeV is 3–5% that of the Crab flux. MGRO J2031+41, detected by the Milagro experiment at 20 TeV (Abdo et al. 2007a), is spatially consistent with the source TeV J2032+4130, while the measured extension is much larger with a diameter of $3.0^\circ \pm 0.9^\circ$. This source is likely to be associated with the pulsar 2FGL

J2032.2+4126, detected by *Fermi* (Abdo et al. 2011).

Evidence of TeV emission at the 4.0 standard deviation (s.d.) level after an X-ray flare from Cyg X-1 was observed by the MAGIC experiment on 2006 September 24 (Albert et al. 2006).

The source VER J2019+407 was discovered in a survey of the Cygnus region by the VERITAS experiment (Weinstein 2009). The measured extensions are $0.16^\circ \pm 0.028^\circ$ and $0.11^\circ \pm 0.027^\circ$ along the major and minor axes, respectively. This source is spatially coincident with the *Fermi* source 2FGL J2019.1+4040, which is potentially associated with a supernova remnant or a pulsar wind nebula (PWN) (Abdo et al. 2011).

During the deep VERITAS observations of the Cyg OB1 region, a point source VER J2016+372 was discovered at the location of CTB 87 (Aliu 2011). The flux is about 1% that of the Crab and the spectral index is about -2.1 from a preliminary analysis.

This region also contains the bright unidentified source MGRO J2019+37, which was detected by the Milagro experiment at 20 TeV (Abdo et al. 2007a) and is the most significant source in the Milagro data set apart from the Crab Nebula. Its extension is $\sigma = 0.32^\circ \pm 0.12^\circ$ in a symmetric two-dimensional Gaussian (Abdo et al. 2007b), which has 68% of the events contained in a region with an angular diameter of $1.1^\circ \pm 0.5^\circ$ (Abdo et al. 2007a). The spectrum of this source is hard with an index of -1.83 and an exponential cutoff at 22.4 TeV (Smith 2010). At the location of MGRO J2019+37, a 2.2 s.d. signal corresponding to 30% Crab unit was observed by the Tibet AS γ experiment (Amenomori et al. 2010). However, about 0.9° away, a possible source was detected (Amenomori et al. 2007). The MGRO J2019+37 is spatially coincident with the *Fermi* source 2FGL J2018.0+3626 and pulsar 2FGL J2021.0+3651 (Abdo et al. 2011). VERITAS has surveyed this region, but no emission from MGRO J2019+37 has been detected (Weinstein 2009). Recently, an in-depth observation of the Cyg OB1 region has been carried out by VERITAS, which unveiled complex TeV emission around MGRO J2019+37 (Aliu 2011).

Among the four known VHE γ -ray sources inside the Cygnus region, MGRO J2019+37 is enigmatic due to its high flux not confirmed by other VHE γ -ray detectors. The measurement of the energy spectrum or an upper limit around several TeV is therefore very useful to understand the nature of the source and its emission mechanism. The ARGO-YBJ experiment is an air shower array with large field of view and can continuously monitor the northern sky. The total exposure to the Crab Nebula reaches about 1200 days and its photon flux has been detected with a statistical significance of 17 s.d. at energies around 1 TeV, which is comparable with the eight-year value of 17.2 s.d. obtained at energies around 35 TeV by Milagro (Abdo et al. 2009). This work presents the observation results for the Cygnus

region, including sources MGRO J2031+41 and MGRO J2019+37, with the ARGO-YBJ experiment.

2. The ARGO-YBJ experiment

The ARGO-YBJ experiment, located in Tibet, China, at an altitude of 4300 m a.s.l., is the result of a collaboration among Chinese and Italian institutions and is designed for VHE γ -ray astronomy and cosmic ray observations. The detector consists of a single layer of Resistive Plate Chambers (RPCs), which are equipped with pick-up strips (6.75 cm \times 61.80 cm each). The logical OR of the signal from eight neighboring strips constitutes a logical pixel (called a “pad”) for triggering and timing purposes. One hundred thirty clusters (each composed of 12 RPCs) are installed to form a carpet of about 5600 m² with an active area of \sim 93%. This central carpet is surrounded by 23 additional clusters (“guard ring”) to improve the reconstruction of the shower core location. The total area of the array is 110 m \times 100 m. More details about the detector and the RPC performance can be found in (Aielli et al. 2006, 2009b).

The ARGO-YBJ detector is operated by requiring the number of fired pads (N_{pad}) at least 20 within 420 ns on the entire carpet detector. The high granularity of the apparatus permits a detailed space-time reconstruction of the shower profile and therefore of the incident direction of the primary particle. The arrival time of the particles is measured with a resolution of about 1.8 ns (Aielli et al. 2009b). In order to calibrate the 18,360 TDC channels, we have developed a method using cosmic ray showers (He et al. 2007). The calibration precision is 0.4 ns and the procedure is applied every month (Aielli et al. 2009a).

The central 130 clusters began taking data in 2006 July, and the “guard ring” was merged into the DAQ stream in 2007 November. The trigger rate is 3.5 kHz with a dead time of 4% and the average duty cycle is higher than 86%. The angular resolution, pointing accuracy and stability of the ARGO-YBJ detector array have been thoroughly tested by measuring the shadow of the Moon in cosmic rays (Bartoli et al. 2011b). The point-spread function (PSF) is quantified using a parameter ψ_{70} as the opening angle containing 71.5% of the events. For $N_{pad} > 1000$, ψ_{70} is 0.47° , while at $N_{pad} \sim 20$ ψ_{70} becomes 2.8° (Bartoli et al. 2011a,b). This measured angular resolution refers to cosmic ray induced air showers, and it is smaller by 30–40% for γ -rays.

3. Data analysis

The ARGO-YBJ data used in this analysis were collected from 2007 November to 2011 August. The total effective observation time is 1182.0 days. To achieve a good angular resolution, the event selections used in (Bartoli et al. 2011a) are applied here and only events with zenith angle less than 50° are used. The total number of events after filtering used in this work is 1.97×10^{11} . The opening angle ψ_{70} for events with $N_{pad} > 60$ is 1.36° . In order to obtain a sky map, an area centered at the source location in celestial coordinates (right ascension and declination) is divided into a grid of $0.1^\circ \times 0.1^\circ$ bins and filled with detected events according to their reconstructed arrival directions. To extract the excess of γ -rays from each bin, the “direct integral method” (Fleysher et al. 2004) is adopted in order to estimate the number of cosmic ray background events in the bin. To remove the effect of cosmic ray anisotropy on a spatial scale of $11^\circ \times 11^\circ$, a correction procedure described in (Bartoli et al. 2011a) has been applied. To take into account the PSF of the ARGO-YBJ detector, the events in a circular area centered on the bin with an angular radius of $1.3\psi_{70}$, are summed together with a weight of the Gaussian-shaped PSF. Equation (17) in (Li & Ma 1983) is used to estimate the significance of the excess in each bin.

With this data analysis, the significance of the excess observed from the direction of the Crab Nebula is 17 s.d., which indicates that the cumulative 5 s.d. sensitivity of ARGO-YBJ has reached 0.3 Crab unit for point sources (Cao & Chen 2011). For an extended source with a symmetric two-dimensional Gaussian shape with $\sigma = 0.32^\circ$, the sensitivity is degraded by a factor of 11%.

4. Results and discussion

The significance map of the Cygnus region as observed by ARGO-YBJ using events with $N_{pad} > 20$ is shown in Figure 1. For comparison, the 4 known TeV sources and 24 GeV sources in the second *Fermi* LAT catalog are marked in the figure. An excess is observed over a large part of the Cygnus region, which indicates a possible diffuse γ -ray emission. An analysis of the diffuse γ -ray emission using ARGO-YBJ data can be found in (Ma 2011). The highest significance value is 6.4 s.d. at $(307.85^\circ, 41.75^\circ)$, consistent with the position of VHE sources MGRO J2031+41 and TeV J2032+4130. No evidence of an emission above 3 s.d. is found at the location of MGRO J2019+37.

4.1. MGRO J2031+41

The intrinsic extension of MGRO J2031+41 is determined by fitting the distribution of θ^2 for the events exceeding the background as shown in Figure 2, where θ is the angular distance of each event to the position of TeV J2032+4130. Only events with $N_{pad} > 60$ are used in this fit, where N_{pad} is the number of fired pads. To fit the data, a set of γ -rays is generated taking into account the spectral energy distribution (SED), the intrinsic source extension, and the detector PSF. The extension is estimated, by minimizing the χ^2 between the data and the generated events, between 0° and 1° with steps of 0.1° . Assuming the background spectral index -2.8 , the intrinsic extension is determined to be $\sigma_{ext} = (0.2_{-0.2}^{+0.4})^\circ$. It is found that the dependence on the SED is negligible within the uncertainties. This result is consistent with the estimation by the MAGIC and HEGRA experiments, i.e., $(0.083 \pm 0.030)^\circ$ and $(0.103 \pm 0.025)^\circ$, respectively.

Assuming an intrinsic extension $\sigma_{ext} = 0.1^\circ$, we estimate the spectrum of MGRO J2031+41 using the ARGO-YBJ data by a conventional fitting method described in (Bartoli et al. 2011a). In this procedure, the expectation function is generated by sampling events in the energy range from 10 GeV to 100 TeV and taking into account the detailed ARGO-YBJ detector response to the events assuming a power law with its spectral index as a parameter. We define four intervals with N_{pad} of 60–99, 100–199, 200–499, and ≥ 500 . The best fit to the SED is shown in Figure 3. The differential flux ($\text{TeV}^{-1} \text{cm}^{-2} \text{s}^{-1}$) in the energy range from 0.6 TeV to 7 TeV is

$$\frac{dN}{dEdAdt} = (1.40 \pm 0.34) \times 10^{-11} \left(\frac{E}{1\text{TeV}}\right)^{-2.83 \pm 0.37}. \quad (1)$$

The integral flux is 31% that of the Crab at energies above 1 TeV, which is higher than the flux of TeV J2032+4130 as determined by the HEGRA and MAGIC experiments, i.e. 5% and 3% Crab unit, respectively. However, this measurement is in agreement with the Milagro new result (Bonamente et al. 2011), also shown in Figure 3.

The reason for the discrepancy between the fluxes measured by Cherenkov telescopes and extensive air shower arrays is still unclear. A contribution is expected from the diffuse γ -ray flux produced by cosmic rays interacting with matter in the Galaxy plane. According to the measurement of diffuse γ -ray flux from the Cygnus region using ARGO-YBJ data (Ma 2011), this contribution to the measured flux from MGRO J2031+41 at energy above 1 TeV is about 10%. Moreover, an estimate of the systematic error is described in (Aielli et al. 2010). With an incomplete list of the sources of systematics, such as the time resolution variation, event rate variation with environment parameters, and pointing error, the error is found to be less than 30%. Due to the limited angular resolution of the ARGO-YBJ detector, nearby sources could contribute to the flux. For TeV J2032+4130, this contribution must

be very small, because there is no source in the $3^\circ \times 3^\circ$ field of view as seen by HEGRA and MAGIC except TeV J2032+4130 itself (Aharonian et al. 2005; Albert et al. 2008). Thus, the contribution from diffuse γ -ray emission, nearby sources, and systematic uncertainty are not enough to explain the discrepancy.

4.2. MGRO J2019+37

No excess above 3 s.d. is detected inside the Cyg OB1 region, even considering extended sources. Taking into account the position uncertainty reported by Milagro, the bin with the maximum significance within 0.3° from MGRO J2019+37 is used to estimate the upper limits. The flux upper limits at 90% confidence level (c.l.) are shown in Figure 4 assuming the SED reported in (Smith 2010) and the extension $\sigma = 0.32^\circ$ given in (Abdo et al. 2007b), respectively. At energies above 5 TeV, the ARGO-YBJ exposure is still insufficient to reach a firm conclusion. As regards the emission at lower energies, the ARGO-YBJ observation does not confirm the spectrum determined by Milagro (Smith 2010). Taking into account that the two observations differ in time by several years, this discrepancy might indicate a variation in the γ -ray flux of the source.

The VERITAS experiment carried out a fine scanning of the Cygnus region. With a sensitivity of about 10% Crab unit, there was no significant signal found in the direction of MGRO J2019+37 (Weinstein 2009). With a deeper survey corresponding to a sensitivity of about 1% Crab unit, some faint sources were found in this region (Aliu 2011). The estimated flux is much weaker than that determined by the Milagro experiment.

Considering the source extension $\sigma = 0.32^\circ \pm 0.12^\circ$ and the distance of the Cygnus region 1–2 kpc, the source radius is estimated to be 4–15 pc, implying that the variation timescale should be longer than 13–49 years. The observation by the ARGO-YBJ experiment is about five years later than that by Milagro. A flux variation over the whole extended region cannot be completely excluded. If the flux variation were dominated by a smaller region in the source area, the picture could be more reasonable. In such a scenario, however, identifying MGRO J2019+37 as a PWN could be a dilemma because it otherwise should have a steady flux.

5. Conclusions

Since 2007 November the ARGO-YBJ experiment is monitoring with high duty cycle the northern sky at TeV photon energies. Using data up to 2011 August, we have observed the Cygnus region, inside which two bright VHE extended γ -ray sources have been detected

by the Milagro experiment. An excess with statistical significance of 6.4 s.d. is detected from the direction of MGRO J2031+41, consistent with the Milagro observation, but with a flux higher than that measured by HEGRA and MAGIC. The source location and extension are, however, consistent with those of TeV J2032+4130. It is not easy to assess the origin of this discrepancy. No signal from MGRO J2019+37 is detected, and the derived upper limits at 90% c.l. are lower than the Milagro flux at energies below 5 TeV. This result could be explained invoking a source variability, making difficult in that case to identify the source as a pulsar wind nebula. In conclusion, further observations and attention to the Cygnus region are needed since it is found to be complex in the VHE domain.

This work is supported in China by NSFC (No.10120130794), the Chinese Ministry of Science and Technology, the Chinese Academy of Sciences, the Key Laboratory of Particle Astrophysics, CAS, and in Italy by the Istituto Nazionale di Fisica Nucleare (INFN).

We also acknowledge the essential supports of W.Y. Chen, G. Yang, X.F. Yuan, C.Y. Zhao, R. Assiro, B. Biondo, S. Bricola, F. Budano, A. Corvaglia, B. D’Aquino, R. Esposito, A. Innocente, A. Mangano, E. Pastori, C. Pinto, E. Reali, F. Taurino and A. Zerbini, in the installation, debugging and maintenance of the detector.

REFERENCES

- Abdo, A. A., Allen, B., Berley, D., et al. 2007a, *ApJ*, 664, L91
- Abdo, A. A., Allen, B., Berley, D., et al. 2007b, *ApJ*, 658, L33
- Abdo, A. A., Allen, B. T., Aune, T., et al. 2009, *ApJ*, 700, L127
- Abdo, A. A., et al. 2011, arXiv:1108.1435v1
- Aharonian, F., Akhperjanian, A., Beilicke, M., et al. 2002, *A&A*, 393, L37
- Aharonian, F., Akhperjanian, A., Beilicke, M., et al. 2005, *A&A*, 431, 197
- Aielli, G., Bacci, C., Bartoli, B., et al. 2006, *Nucl. Instrum. Meth. A*, 562, 92
- Aielli, G., Assiro, R., Bacci, C., et al. 2009a, *Astrop. Phys.*, 30, 287
- Aielli, G., Bacci, C., Bartoli, B., et al. 2009b, *Nucl. Instrum. Meth. A*, 608, 246
- Aielli, G., Bacci, C., Bartoli, B., et al. 2010, *ApJ*, 714, L208

- Albert, J., Aliu, E., Anderhub, H., et al. 2006, *ApJ*, 665, L51
- Albert, J., Aliu, E., Anderhub, H., et al. 2008, *ApJ*, 675, L25
- Aliu, E., 2011, in Proc. 32nd ICRC, in press (available at <http://icrc2011.ihep.ac.cn>)
- Amenomori, M., Bi, X. J., Chen, D., et al. 2007, in Proc. 30th ICRC, ed. R. Caballero et al. (Mexico City: Univ. Nacional Autonoma de Mexico), 695 (available at <http://www.icrc2007.unam.mx/proceedings>)
- Amenomori, M., Bi, X. J., Chen, D., et al. 2010, *ApJ*, 709, L6
- Bartoli, B., Bernardini, P., Bi, X. J., et al. 2011a, *ApJ*, 734, 110
- Bartoli, B., Bernardini, P., Bi, X. J., et al. 2011b, *Physical Review D*, 84, 022003
- Bonamente, E., Galbraith-frew, J., Hüntemeye, P. 2011, in Proc. 32nd ICRC, in press (available at <http://icrc2011.ihep.ac.cn>)
- Cao, Z., & Chen, S.Z. 2011, in Proc. 32nd ICRC, in press (arXiv:1110.1809v1)
- Fleysher, R., Fleysher, L., Nemethy, P., et al. 2004, *ApJ*, 603, 355
- He, H. H., Bernardini, P., Calabrese Melcarne, A. K., & Chen, S. Z. 2007, *Astropart. Phys.*, 27, 528
- Hunter, S. D., Bertsch, D. L., Catelli, J. R., et al. 1997, *ApJ*, 481, 205
- Konopelko, A., Atkins, R. W., Blaylock, G., et al. 2007, *ApJ*, 658,1062
- Li, T.P.,& Ma, Y.Q. 1983, *ApJ*, 272, 317
- Ma, L.L. 2011, in Proc. 32nd ICRC, in press (available at <http://icrc2011.ihep.ac.cn>)
- Smith, A.J. 2010, in Proc. Fermi Symposium (available at <http://www.slac.stanford.edu/econf/C0911022>) (arXiv:1001.3695v1)
- Weinstein, A. 2009, in Proc. Fermi Symposium (available at <http://www.slac.stanford.edu/econf/C0911022>) (arXiv:0912.4492v1)

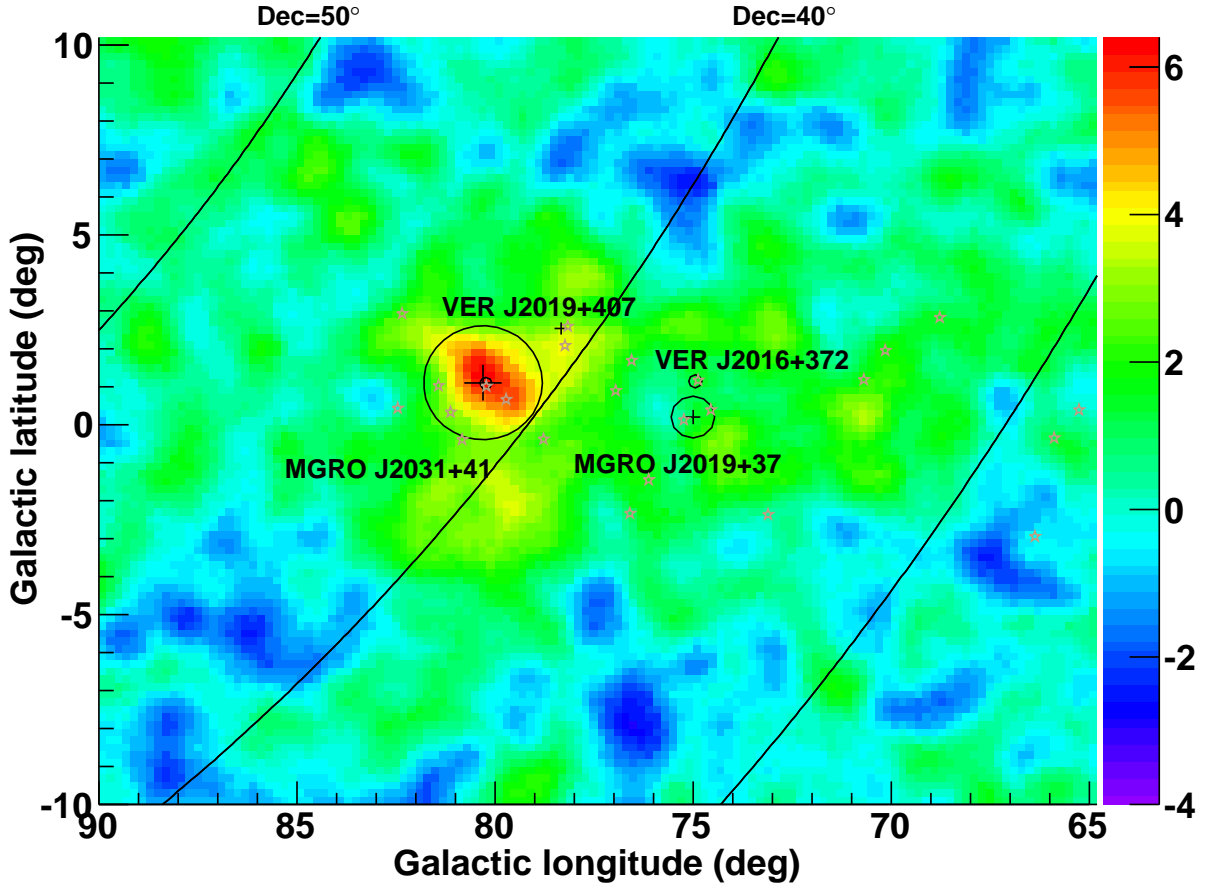


Fig. 1.— Significance map of the Cygnus Region as observed by the ARGO-YBJ experiment. The four known VHE γ -ray source are reported. The errors on the MGRO source positions are marked with crosses, while the circles indicate their intrinsic sizes (Abdo et al. 2007a,b). The cross for VER J2019+407 indicates its extension (Weinstein 2009). The source VER J2016+372 is marked with small circles without position errors. The small circle within the errors of MGROJ2031+41 indicates position and extension of the source TeV J2032+4130 as estimated by the MAGIC collaboration (Albert et al. 2008). The open stars mark the location of the 24 GeV sources in the second *Fermi* LAT catalog.

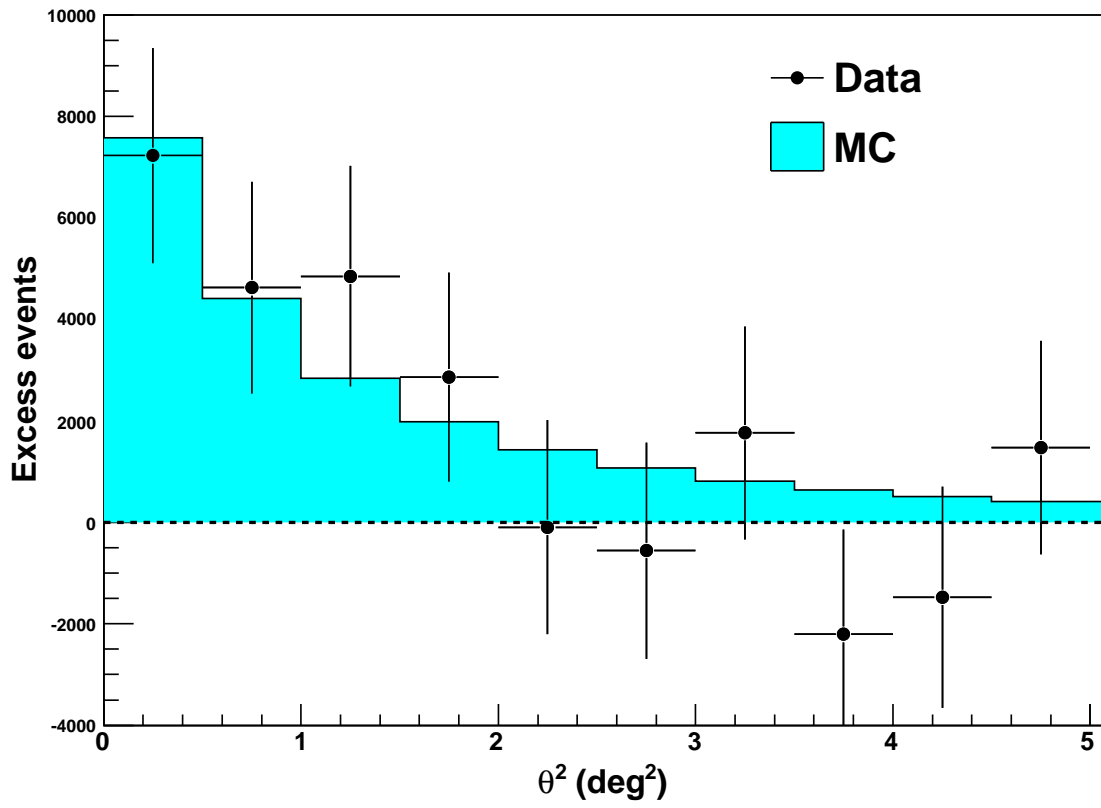


Fig. 2.— Distribution of θ^2 for the number of excess events around TeV J2032+4130. The filled region is the best fit to simulated data.

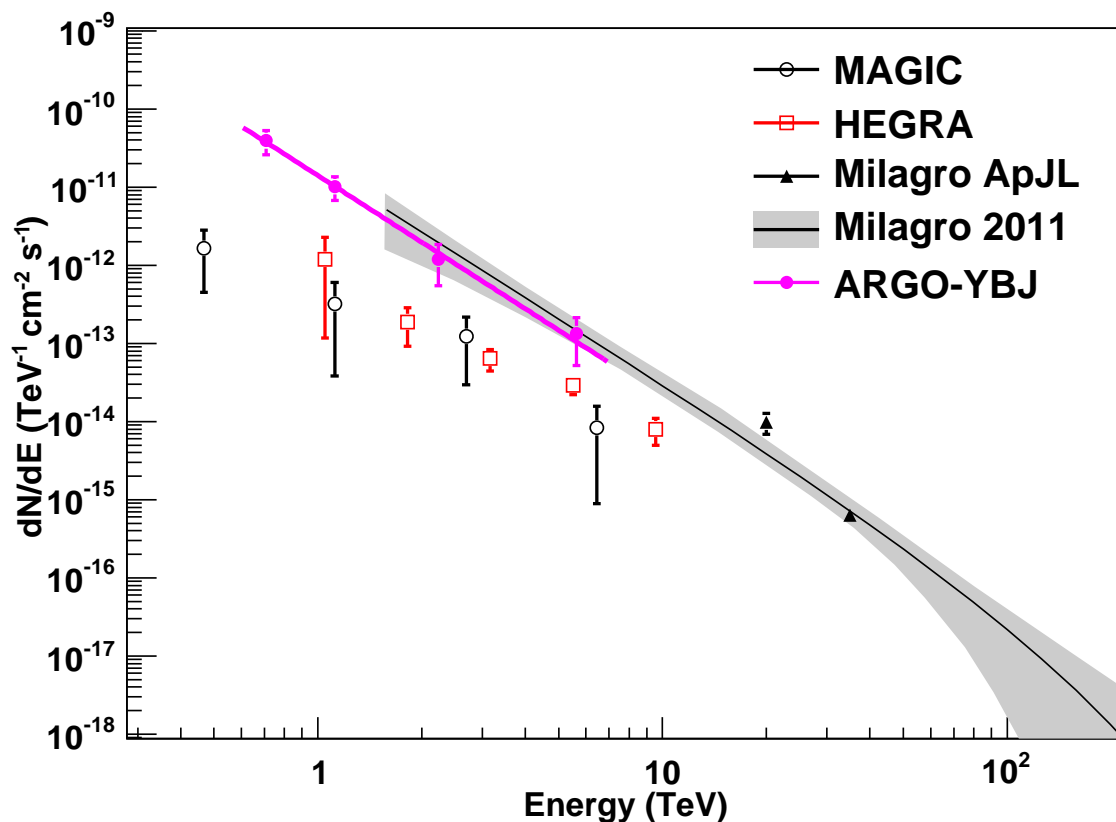


Fig. 3.— Energy density spectrum from TeV J2032+4130/MGRO J2031+41 as measured by the ARGO-YBJ experiment (magenta solid line). The spectral measurements of HEGRA (Aharonian et al. 2005) and MAGIC (Albert et al. 2008) are also reported for comparison. The solid line and shaded area indicate the differential energy spectrum and the 1 s.d. error region as recently determined by the Milagro experiment (Bonamente et al. 2011). The two triangles give the previous flux measurements by Milagro at 20 TeV (Abdo et al. 2007a) and 35 TeV (Abdo et al. 2009).

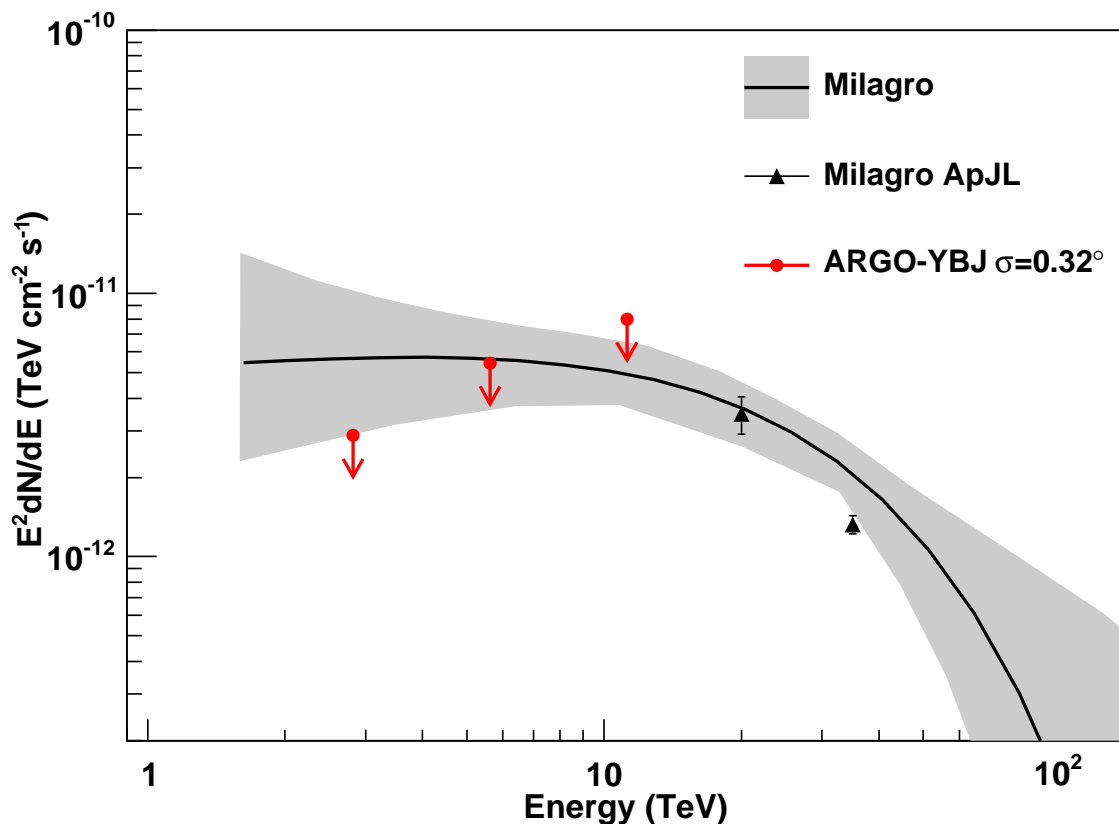


Fig. 4.— Upper limits to the flux from MGRO J2019+37 derived by the ARGO-YBJ experiment adopting the spectrum given in (Smith 2010). The extension is assumed to be $\sigma = 0.32^\circ$ as given in (Abdo et al. 2007b). The solid line and shaded area indicate the differential energy spectrum and the 1 s.d. error region as determined by the Milagro experiment (Smith 2010). The two triangles give the previous flux measurements by Milagro at 20 TeV (Abdo et al. 2007a) and 35 TeV (Abdo et al. 2009).